

International Journal of Nanoelectronics and Materials

IJNeaM ——

ISSN 1985-5761 | E-ISSN 2232-1535



Boosting the structural, optical and AC electrical characteristics of PVA/CdTe nanocomposites for flexible smart optoelectronic devices

Kadhim K. Kadhima, Halah Mohammed Azeeza, Reem Tuama Yousifb, Musaab Khudhur Mohammeda, Mohanad H. Meteab c*

- ^aDepartment of Physics, College of Education for Pure Sciences, University of Babylon, Babylon 51002, Iraq
- ^bDepartment of Physics, College of Sciences, University of Babylon, Babylon 51002, Iraq
- ^cGeneral Directorate of Education in Babylon Governorate, Ministry of Education, Babylon 51001, Iraq
- * Corresponding author. Tel.: +9647812994554; e-mail: mohanad.h.meteab87@gmail.com

Received 23 November 2024, Revised 18 March 2025, Accepted 16 April 2025

ABSTRACT

This research intends to create cadmium telluride nanoparticles (CdTe NPs) and polyvinyl alcohol (PVA) nanocomposites using the casting process to improve structural, AC electrical, and optical properties. To characterize the films, Fourier-transform infrared (FTIR) spectroscopy, UV-visible spectroscopy, and alternating current (AC) electrical characteristics are implemented. The FTIR study indicates a complicated interaction between the PVA matrix and CdTe nanoparticles. The optical band gap diminishes and absorbance increases with higher concentrations of CdTe nanoparticles in the PVA matrix. Further improvements have been made to the polymer films' extinction factor, reflecting index, optical conductivity, and dielectric properties. The dielectric constant and dielectric loss increased with the frequency and concentration of CdTe nanoparticles, according to the AC electrical properties. Conversely, the electrical conductivity of AC current rises with the frequency and concentration of CdTe nanoparticles, increasing by 55.02% at a frequency of 100 Hz. Ultimately, these findings indicate that the PVA/CdTe nanocomposite is applicable in photodetector devices.

Keywords: Nanocomposites; PVA/CdTe; FTIR; Optical properties; AC electrical characteristics; Bandgap energy

1. INTRODUCTION

Nanomaterials are frequently used with bulk polymeric materials to enhance their properties because of their remarkable qualities. Materials that contain nanoparticles are termed nanocomposites. Based on the material used for the matrix, nanocomposites can be classified as metallic matrix composite materials, ceramic matrix material composites, or composites with a polymer matrix. The arrangement of nanofillers within the bulk polymer matrix is the primary factor in the production of polymer matrix composites [1]. Homogeneous dispersion of nanoparticles leads to better properties. Nonetheless, the weak van der Waals interactions among the nanomaterials promote aggregation, thereby undermining characteristics. It has recently been demonstrated that adding a compatibilizer also enhances the nanoparticles' dispersion within the polymer matrix [2]. Enhancing the outer layer of nanomaterials through modification and functionalization leads to improved interfacial interactions or connections between the filler and matrix. This consequently enhances dispersion and facilitates more efficient transfer of strain within a matrix and filler. The final outcome is a set of high-performance, lightweight composites that are perfectly suited for advanced applications [3].

Recently, there has been a rise in interest in the production of II-VI semiconductor nanoparticles [4]. Nanocrystalline semiconductor films' distinct nonlinear visual effects and quantum confinement make them a novel layer of photonic

material [5]. The precursor of II-VI semiconductor materials, cadmium telluride nanoparticles (CdTe NPs) are thought to have a variety of sophisticated applications, from fluorescent materials to microelectronics. This is because of its high photovoltaic synthesis capacity, which is achieved by controlling the particle's size, surface, and shape in the quantum confinement regime [6]. A variety of studies have explored CdTe nanoparticles. CdTe nanoparticles are employed in solid-state lighting, exhibits, communication via optical fiber, sensors, solar cells, and medical imaging and detection due to their high quantum yield and availability in multiple colors [7-9]. Excellent optical qualities, moderate conductivity, and affordability are all well-balanced in CdTe. When compared to substitutes like ZnO, TiO2, and PbS, which either have limits in optical absorption or raise environmental concerns, it is still a desirable option for optoelectronics and nanocomposite applications despite toxicity concerns. CdTe is a desirable material for solar cells, light-emitting diodes (LEDs), and photodetectors because of its capacity to control the bandgap, produce high quantum yields, and preserve The best mix of visible light absorption, photoluminescence, and quantum confinement makes CdTe a better option than other semiconductor nanoparticles for your particular application (e.g., CdTe-PVA composites for optoelectronic and antibacterial applications) [7]. Polyvinyl alcohol (PVA), a semicrystalline polymer, is an excellent host matrix for CdTe nanostructures because it is chemically resistant, has strong mechanical properties (film

formation), is water soluble, and has modest electrical resistance (depending on dopants) [8,9]. This significant substance has several uses in a variety of scientific and technological domains. Because of the hydrogen bonds that occur between the hydroxyl groups, PVA's polymer chains interact strongly with one another. These hybrid materials offer a wider range of applications since metal nanoparticles doped in polymers are highly desirable. The crystal structure of PVA is altered following its creation on a composite with NPs, as demonstrated by Liu et al. [10]. In PVA/CdTe nanocomposites, you can investigate quantum confinement effects, interfacial polarization, and charge transport mechanisms to improve the theoretical explanation of the observed behaviors (such as optical bandgap reduction, dielectric behavior, and AC conductivity trends). The phenomenon of semiconductor nanoparticles' optical and electrical characteristics changing when their size is reduced to the nanoscale (usually less than 10 nm) is known as quantum confinement. Regarding CdTe nanoparticles, this confinement results in: Expansion/Reduction: The energy gap between the valence and conduction bands may widen or contract as the particle size reduces, contingent on the particle size. Reduced particle size for CdTe frequently causes a red shift (reduction in bandgap) for smaller particles and a blue shift (increase in bandgap) for larger particles [11–14].

The dielectric behavior of the nanocomposite is substantially governed by the interface between the CdTe nanoparticles and the PVA polymer matrix. This phenomenon is referred to as interfacial polarization. When there is a higher concentration of CdTe doping, the interfacial polarization becomes more apparent: High Doping Concentration: When CdTe nanoparticles are equally dispersed throughout the polymer matrix, they produce zones at the interfaces where they exhibit unique polarization features. This occurs when the doping concentration is high. There is a possibility that this will result in higher dielectric constants and a more evident AC conductivity [15].

The charge transport mechanism in semiconductorpolymer nanocomposites is influenced by a number of factors, including the percolation threshold, electron hopping, and charge trapping at interfaces. Those Electrons That Hop: At lower doping concentrations, the majority of the charge transfer occurs as a result of electron hopping between CdTe nanoparticles. This results in an increase in the composite's total conductivity. A threshold for the process of percolation. In the event that a threshold concentration of nanoparticles is reached, the construction of a percolative conduction network makes it possible for charge transfer to be carried out with greater efficiency. On the other hand, charge trapping may occur as a consequence of nanoparticle aggregation at high concentrations, which may potentially result in a reduction in conductivity [16]. In this present study, we delve into the advanced characteristics of PVA/CdTe nanocomposites, leveraging state-of-the-art techniques including Fourier Transform Infrared (FTIR) spectroscopy, Ultraviolet-Visible-Near Infrared (UV-Vis-NIR) spectroscopy, and alternating

electrical property analysis to evaluate their promise for innovative smart optoelectronic applications.

2. MATERIALS AND METHODS

Using a casting method, films of PVA/CdTe nanocomposites were made with different amounts of cadmium telluride (CdTe) nanopowder (CdTe, purity 99.99%, 60-70 nm, amorphous), which was bought from US Research Nanomaterials, Inc. 1 gram of PVA was mixed with 50 milliliters of deionized water to make the film. A magnetic stirrer was utilized to homogenize the polymers and enhance the fluid's uniformity. The CdTe nanoparticles were incorporated into the PVA solution at amounts of 1%, 3%, and 5%. Nanocomposites of polyvinyl alcohol (PVA) and cadmium telluride (CdTe) were combined and fabricated into films with a thickness of 110 µm. Infrared Fourier Transform Spectroscopy (FTIR) is a technique used for obtaining an infrared spectrum of absorption or emission of a solid, liquid, or gas. The device was designed to analyze structural features by covering the spectral range from 500 to 4000 cm⁻¹. The PVA/CdTe nanocomposites were analyzed optically using a UV-18000A-Shimadzu spectrophotometer. The electrical characteristics of PVA/CdTe nanocomposites were evaluated utilizing an LCR meter (HIOKI 3532-50 LCR HI TESTER) across a frequency range of 100 Hz to 5 MHz.

3. RESULT AND DISCUSSION

The FTIR spectra demonstrate the rotational and vibrational characteristics of a substance's chemical groupings. Figure 1 illustrates the FTIR properties of the PVA/CdTe nanocomposites across a wave number range of 500–4000 cm⁻¹. The FTIR spectra of pure PVA polymer, as shown in image (A), display an absorbance band at 3264 cm⁻ ¹, which is related to 0-H stretching vibrations, and a different one at 2920 cm⁻¹, linked to the asymmetric stretching of CH₂. The band at 1261 cm⁻¹ is believed to originate from the C-O stretching vibration. The absorbed bands observed at 1595 cm⁻¹ correspond to the C=0 carbonyl stretch. The bands identified at 1418 cm⁻¹ and 1084 cm⁻¹ are associated with the stretching of CO and the bending of OH, respectively. The absorbing band observed at 837 cm⁻¹ is associated with the C-C stretching vibration [17,18].

The spectra presented in images B, C, and D illustrate the variations in PVA spectra corresponding to different concentrations of CdTe NPs. The spectra exhibit the presence of CdTe NPs, indicating a shift in specific bands and a variation in certain intensities. FTIR analysis indicates that the introduction of varying quantities of CdTe NPs in images B, C, and D results in a shift of certain bonds, while no new peaks are formed. Subsequently, there is physical interaction between the CdTe nanoparticles and the PVA polymer matrix. These findings agree with researchers [19]. Figure 2 shows the wavelength-absorption relationship of (PVA/CdTe) nanocomposites. According to the figure, all samples absorb more UV light. Stimulating the donor's electrons raised their energy. Additionally, the results demonstrated that the samples absorbed a sizable number of photons in the ultraviolet range. A graphic illustrating the

effect of load ratio and CdTe NPs on absorbance is included in the analysis. As the load ratio was increased from 1 wt.% to 5 wt.%, the system's absorbance demonstrated a direct correlation with the CdTe NPs ratio. A greater concentration of charged carriers could be the cause of the absorbance rise. The observed behaviors may be explained by the limited ability of compressed photons to interact with atoms, possibly due to their low energy levels and longer wavelength of propagation. This outcome is in line with study findings [20–22].

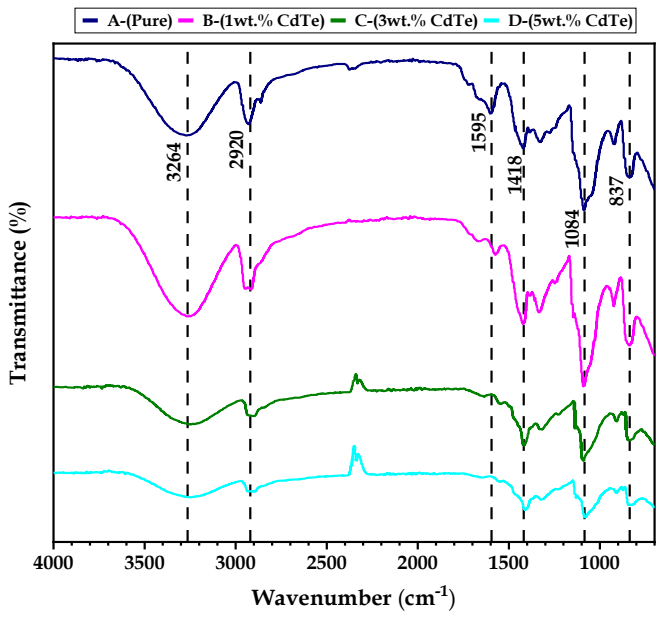


Figure 1. FTIR spectra for (PVA/CdTe) nanocomposites:(A) for pure PVA, (B) for 1 wt.% CdTe NPs, (C) for 3 wt.% CdTe NPs and (D) for 5 wt.% CdTe NPs

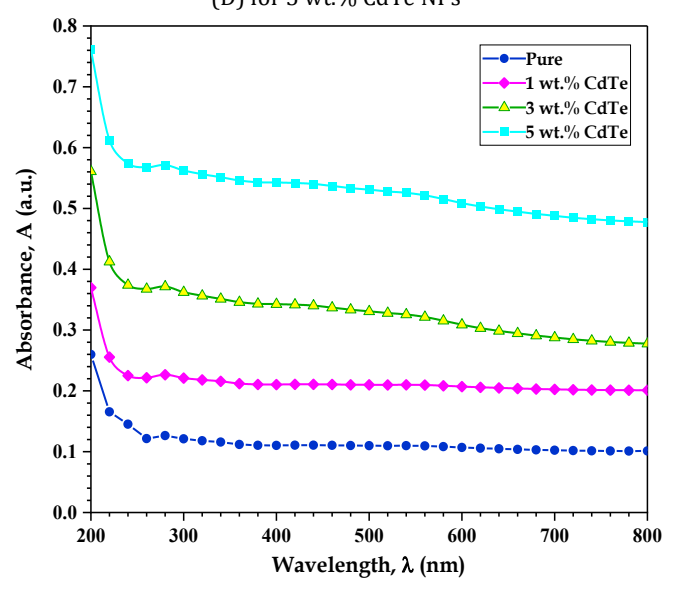


Figure 2. Absorbance of PVA/CdTe nanocomposites with wavelength

Figure 3 illustrates the transmission properties of the PVA/CdTe nanocomposite with varying amounts of CdTe NPs. The figure demonstrates a reduction in transmittance with a rise in the ratio of CdTe NPs. The rise in surface roughness is due to the accumulation of nanoparticles. The dispersion of light is increased due to the heightened surface fragmentation. Although there may be financial implications, the nanocomposite films have decreased UV

wavelength transmission, making them ideal for pharmaceutical packaging because of their absorption feature [23,24].

The absorption coefficient (α) is determined through calculation [25]:

$$\alpha = 2.303 \, (A/d)$$
 (1)

Where A is absorbance and d is sample thickness. The PVA/CdTe nanocomposite absorbance coefficient is shown in Figure 4. The chart shows that all samples' absorbance coefficients increase proportionally with increasing CdTe NP concentrations. This increases the nanocomposites' electric charge conduction. All of the samples' absorption coefficients exhibit low values at low energies, suggesting that there is little chance of electron migration. As the energy of the input photon increases, these coefficients demonstrate an upward trend, indicating a greater probability of electron transference. This suggests that the resulting photons have adequate energy to interact with the elements effectively. The measured α values of the generated films, which fall below 104 cm⁻¹, indicate the potential for indirect electronic transitions. The results support the researchers' findings [26,27].

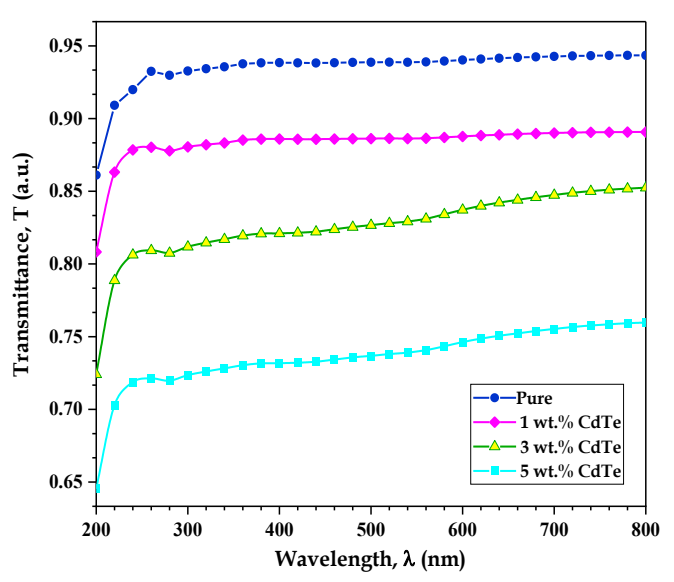


Figure 3. Transmittance of PVA/CdTe nanocomposites with wavelength

The energy gap is given by [28]:

$$(\alpha h \upsilon)^{1/m} = C(h \upsilon - E_g) \tag{2}$$

For any constant C, the photon energy is characterized by the symbol hu, the energy gap is represented by the symbol Eg, and the value of m can alternate between two and three for indirect transitions that are permitted and those that are prohibited, respectively. Both Figure 5 and Figure 6 illustrate the indirect band gap that is present in the PVA/CdTe nanocomposite. Employing the interruption of the larger line segment. A segment of the curve depicted in Figures 6 and 7 was extracted to construct a linear representation of the energy gap. The graph demonstrates that an increase in the amount of CdTe nanoparticles leads to a notable decrease in the energy gap. The energy

separation of the valence and the conducting bands in PVA/CdTe nanocomposites reduces from 3.85 eV in pure PVA to 3.118 eV. The forbidden band gap, characterized as the energy variance between the valence band and the conduction band, reduced from 2.82 eV for PVA polymers to 1.718 eV for PVA/CdTe nanocomposites by adjusting the polymer quantity and elevating the loading ratio from 0 wt.% to 5 wt.% resulted in a drop in value. The behavior seen is caused by changes in the amounts of parity and delivery packages in certain areas. The arrangement of connection package levels is in line with what different academic studies have found. In Table 1, explain the values of allowed and forbidden energy gaps. This finding agrees with what researchers found [29].

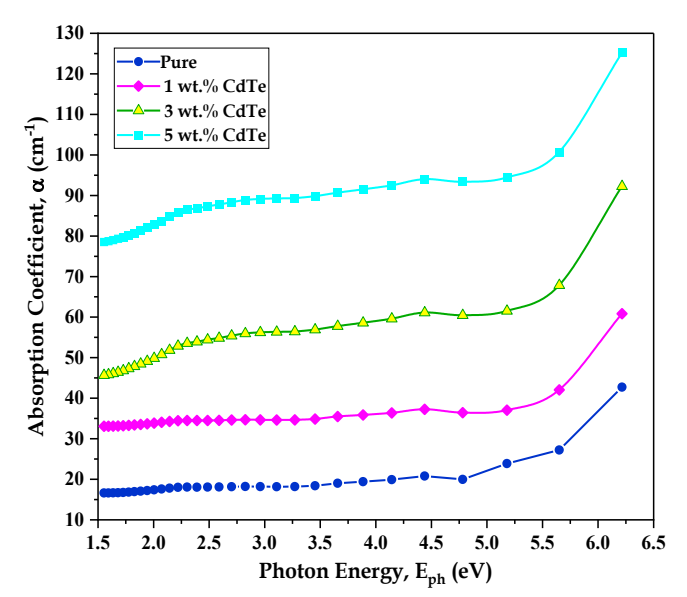


Figure 4. Absorption coefficient with photon energy of PVA/CdTe nanocomposites

The extinction coefficient (k) is determined by [30]:

$$k = \alpha \lambda / 4\pi$$
 (3)

where λ is the wavelength, and the absorption coefficient (k) of PVA/CdTe nanocomposites is revealed in Figure 7. This graph shows that as the wavelength goes up, the extinction coefficient of the PVA/CdTe nanocomposites goes up too. This behavior might be because photon energy is going up at the same time. It is easy to see that the absorption coefficient of nanocomposites is related to the concentration ratio of CdTe NPs. It is possible that this happens because more light is being absorbed [29,31].

The refractive index (n) is determined by [32]:

$$n = (1 + \sqrt{R})/(1 - \sqrt{R})$$
 (4)

Wherever R represents the reflectance in this context. A representation of the refractive index (n) of the PVA/CdTe nanocomposites can be found in Figure 8. This image demonstrates that the index of refraction for PVA/CdTe nanocomposites has a distinct peak at lower energies, particularly at 240 nm, and then it decreases as the energies increase. This specific peak is particularly noticeable at 240 nm. In addition to this, it has been shown that the refractive index increases in proportion to the rising concentration

ratio of CdTe nanoparticles. The phenomenon that was observed can be attributed to the contemporaneous rise in the density of the nanocomposite [33].

Table 1: The parameters of the tapered fibre

CdTe-doped PVA (wt.%)	Allowed Eg (eV)	Forbidden Eg (eV)
0	3.850	2.820
1	3.491	2.279
3	3.118	1.718
5	2.301	0.523

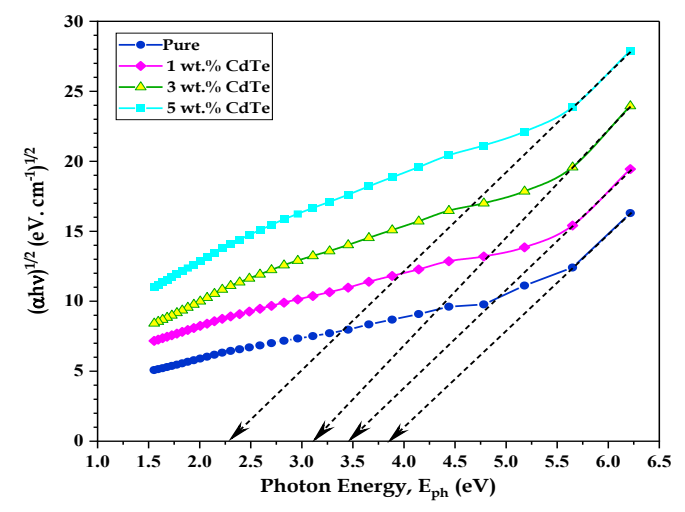


Figure 5. $(\alpha h \upsilon)^{1/2}$ variation with photon energy for PVA/CdTe nanocomposites

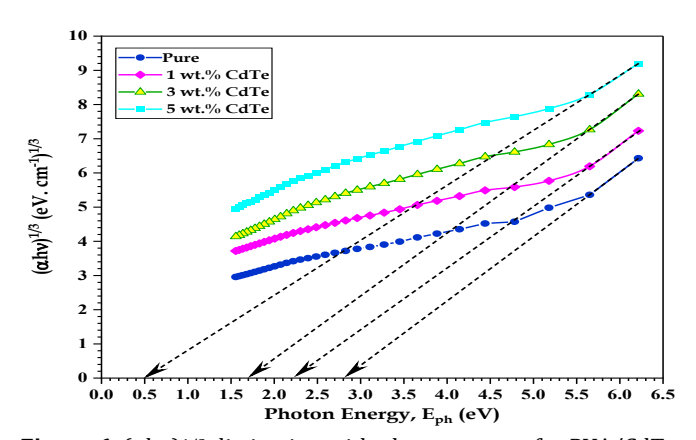


Figure 6. (αhυ)^{1/3} distinction with photon energy for PVA/CdTe nanocomposite

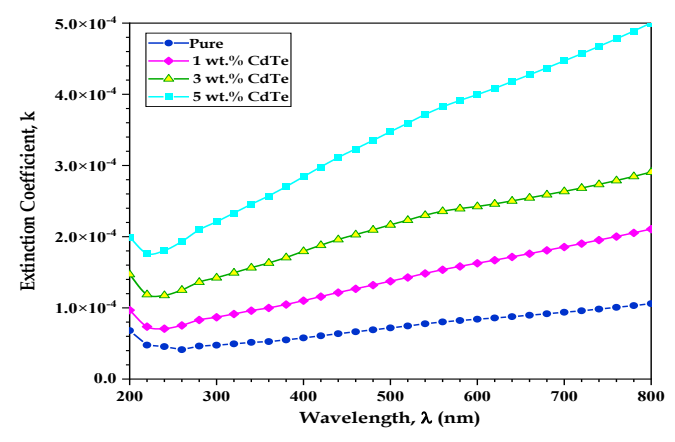


Figure 7. Extinction coefficient disparity with wavelength for PVA/CdTe nanocomposites

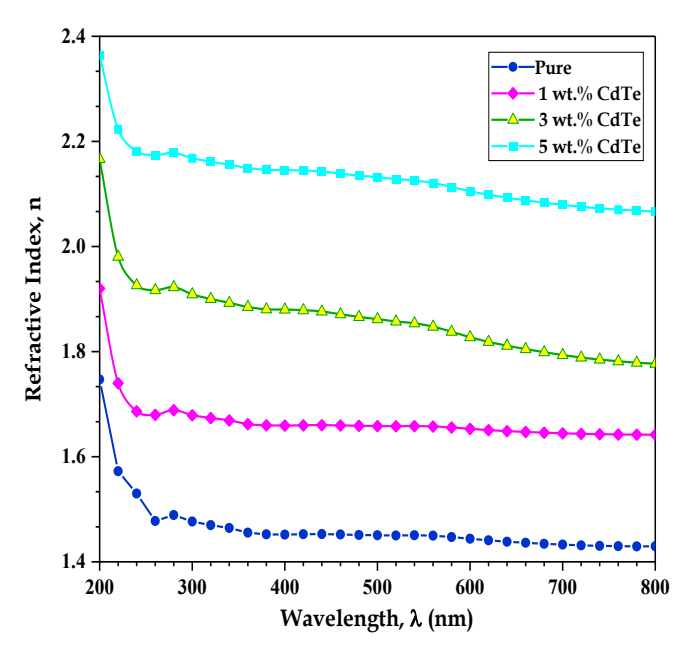


Figure 8. Refractive index variation with wavelength for PVA/CdTe nanocomposites

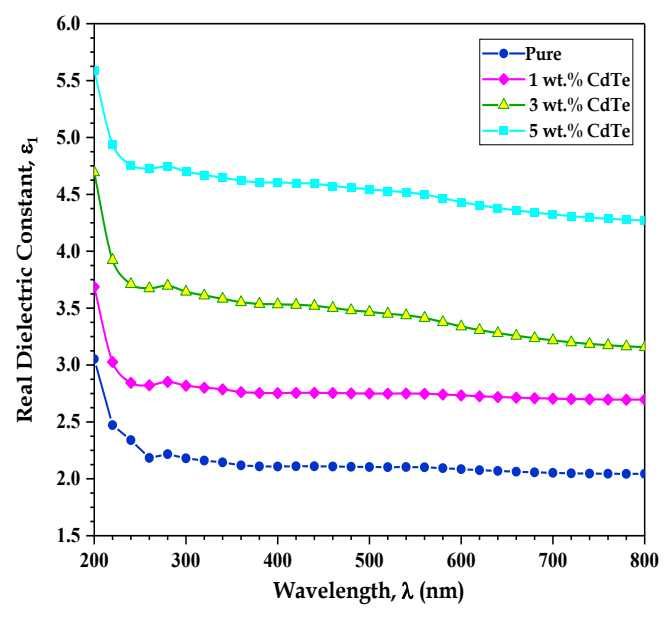


Figure 9. Fluctuation of the real part of the dielectric constant in PVA/CdTe nanocomposites as a function of wavelength

The dielectric constant consists of two components: the real component (ϵ_1) and the imaginary component (ϵ_2) [34]:

$$\varepsilon_1 = n^2 - k^2 \tag{5}$$

$$\varepsilon_2 = 2nk$$
 (6)

Figures 9 and 10 illustrate the variations in the real (ϵ_1) and imaginary (ϵ_2) components of the dielectric constant for the PVA/CdTe nanocomposite as a function of wavelength. This graph shows that as the CdTe NPs level rose, the real and imaginary parts grew. The observed resemblance can be attributed to the greater influence of (n) values on the effective dielectric constant compared to (k) values, as (k) values are significantly smaller than the refractive index, particularly when squared. This finding agrees with what researchers found [35,36].

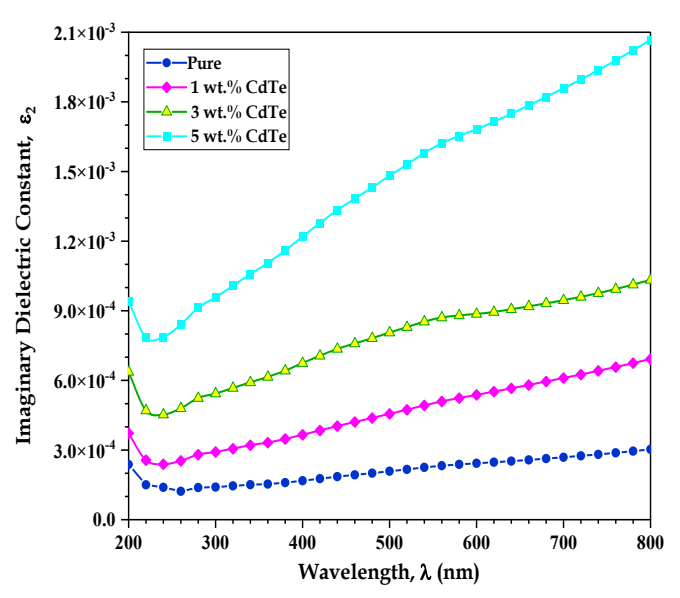


Figure 10. The imaginary part of the dielectric constant fluctuates with wavelength in PVA/CdTe nanocomposites

The optical conductivity (σ_{op}) is defined by [37]:

$$\sigma_{\rm op} = \alpha nc/4\pi$$
 (7)

Where c is the speed of light. Figure 11 shows how the optical conductivity of the PVA/CdTe mixture changes with wavelength. A noticeable increase in optical conductivity is observed at lower wavelengths for the PVA/CdTe nanocomposites. This is followed by a decrease at longer wavelengths. The rise in the absorption rate at the same time can explain this behavior [38]. A direct link was found between the amount of CdTe NPs present and the optical conductivity that was measured. The rise in the absorption rate can be linked to the things that have been seen. This finding agrees with what researchers found [39].

The dielectric constant is calculated using the following equation [40]:

where Cp represents the capacitance of the material, d denotes thickness (in cm), and A signifies area (in cm²). Figure 12 illustrates the variation of the dielectric constant with frequency for polymer blends (PVA/CdTe) and their nanocomposite films containing varying concentrations (1 wt.%, 3 wt.%, and 5 wt.%) of CdTe nanoparticles. This figure shows that space charge polarization decreased relative to total polarization, lowering dielectric constant values for all samples with increasing frequency. This suggests that space charge polarization plays a more significant role in the total polarization at lower frequencies. Figure 13 demonstrates the connection between the dielectric constant and the ratio of CdTe nanoparticles at a frequency of 100 Hz. The illustration illustrates the development of the dielectric constant in nanocomposites as the CdTe content increases. At a frequency of 100 Hz, the highest concentration of CdTe resulted in a 40.96% increase in dielectric constant compared to the pure polymer. The noted phenomenon relates to the interfacial polarization occurring in

nanocomposites when exposed to an alternating electric field, alongside the increase in charge carriers [41].

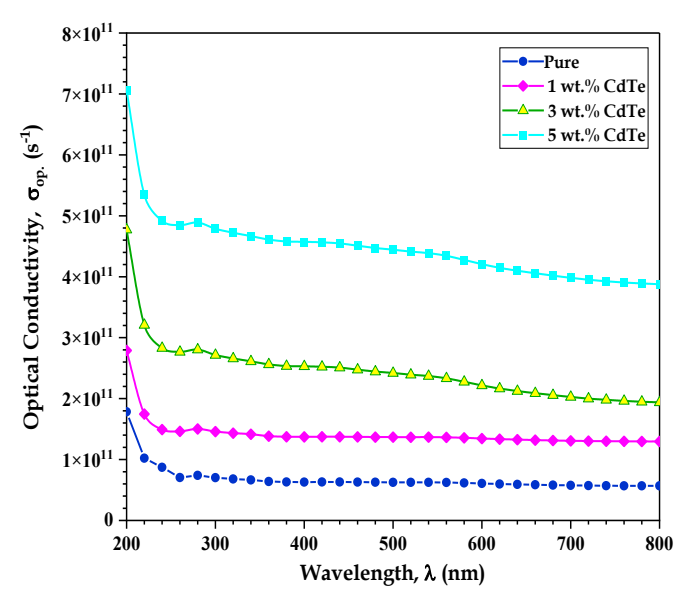


Figure 11. Exploring the wavelength dependence of optical conductivity in PVA/CdTe nanocomposites

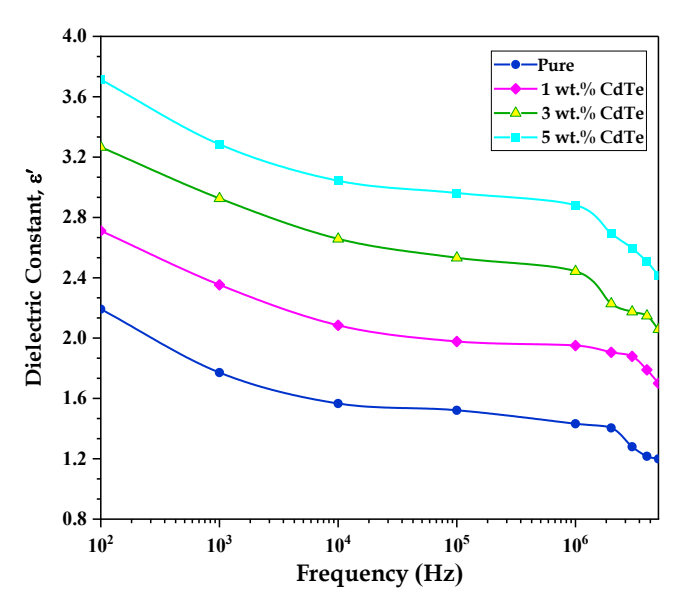


Figure 12. Frequency-dependent dielectric constant for PVA/CdTe nanocomposites at RT

The following equation calculates nanocomposites' dielectric loss [42]:

$$\varepsilon'' = \acute{\epsilon} D$$
 (9)

Which, D: dispersion factor. Figure 14 shows how the dielectric loss and electric field frequency of CdTe in the PVA polymer change with temperature at room temperature (RT). All samples show that increasing the frequency of the electric field leads to a decrease in the dielectric loss of the nanocomposites. The reason for this behavior is that space charge polarization is becoming less important. Also, the nanocomposite films with 5% CdTe show the highest dielectric loss of 0.33 at 10^2 Hz, which is a very low frequency. Figure 15 illustrates that an increase in nanoparticle concentration correlates with an elevation in the dielectric loss of CdTe-based nanocomposites. This

pertains to augmenting the quantity of charge carriers. Identical behavior was documented in [43].

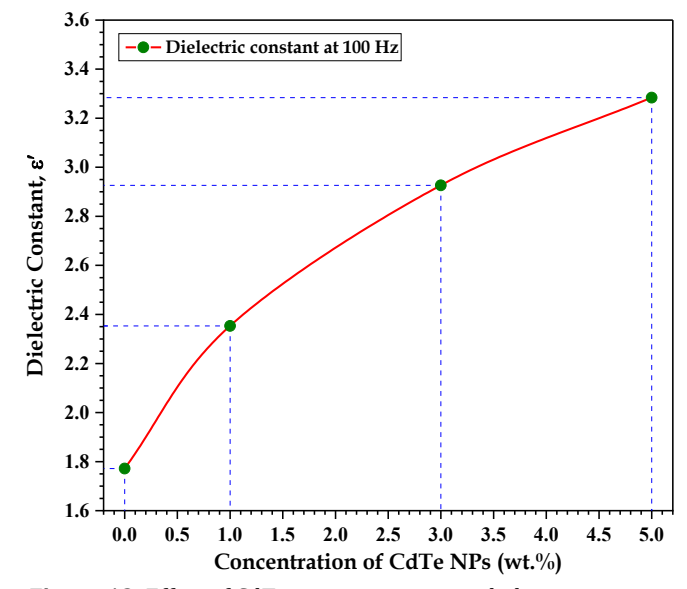


Figure 13. Effect of CdTe concentrations on dielectric constant for (PVA/CdTe) nanocomposites at 100Hz

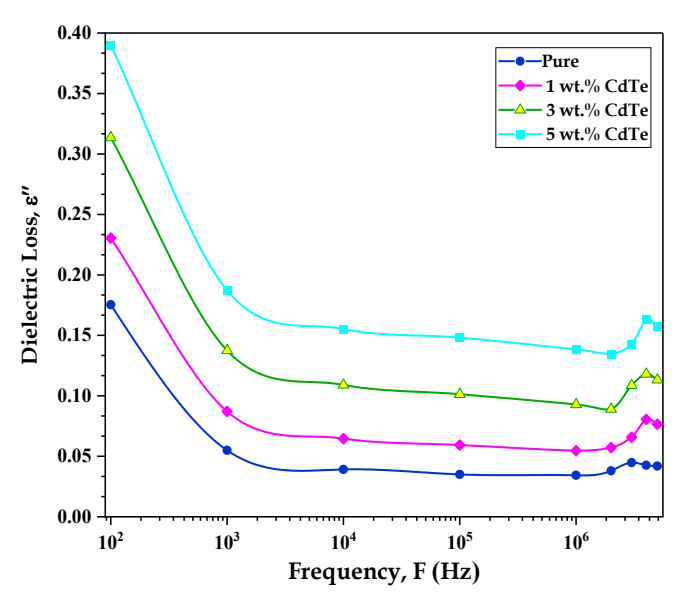


Figure 14. Variation of dielectric loss for (PVA/CdTe) nanocomposites with frequency at RT

The AC electrical conductivity of nanocomposites is calculated by using the following equation [43]:

$$\sigma_{AC}=2\pi f \, \dot{\epsilon} \, D \, \epsilon_o$$
 (10)

Figure 16 illustrates the variation of A.C. conductivity of electricity with the frequency of the electrical field for CdTe in PVA polymers at room temperature (RT). For all samples, the A.C. conductivity goes up a lot as the frequency of the electric field goes up. Charge transmitters move through a process known as "hopping," which is connected to the low-frequency polarization of charged particles and this impact. We also found that the conductance of the PVA/CdTe nanocomposite at 100 Hz increases as the weight percentage of CdTe increases, as shown in Figure 17. The conductivity of the nanocomposite goes up when nanoparticles are added because they increase the number of charge carriers. Because of this, the nanocomposite's

resistance goes down, and its ability to carry AC electricity goes up. The same kind of behavior was recorded in [44].

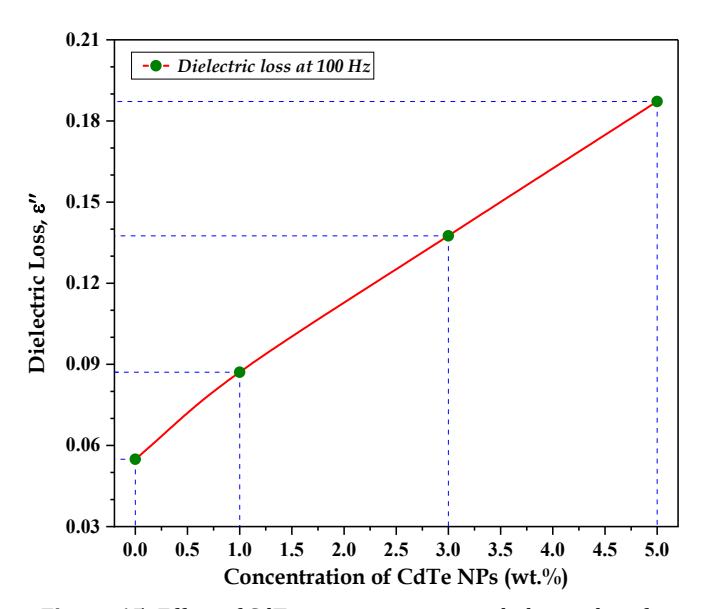


Figure 15. Effect of CdTe concentrations on dielectric loss for (PVA/CdTe) nanocomposite at 100Hz

Table 2 Comparative analysis of CdTe-PVA composites with existing studies

Property	Р.	S. Tewari <i>et</i>	This
Troperty	Chowdhury (2009) [45]	al. (2020) [46]	Study (CdTe- PVA)
Dielectric Constant	Saturation beyond 3% doping	Enhanced with doping, but saturation at higher concentration s	Increases with doping (1–5%)
Optical Absorption	Conductivity increases at low doping, drops at higher levels.	Conductivity improves, but high doping causes charge trapping.	Enhanced with increased doping
Electrical Conductivity	Charge hopping conduction, trapping at higher doping	Enhanced charge transport at low doping decreases with higher doping.	Increases with doping, no drop at 5%
Charge Transport Mechanism	Not analyzed for high- frequency behavior	Frequency- dependent dielectric behavior observed	Likely improved hopping conductio n
Frequency Dependence of ε'	Saturation beyond 3% doping	Enhanced with doping, but saturation at higher concentration	Stable across frequency range

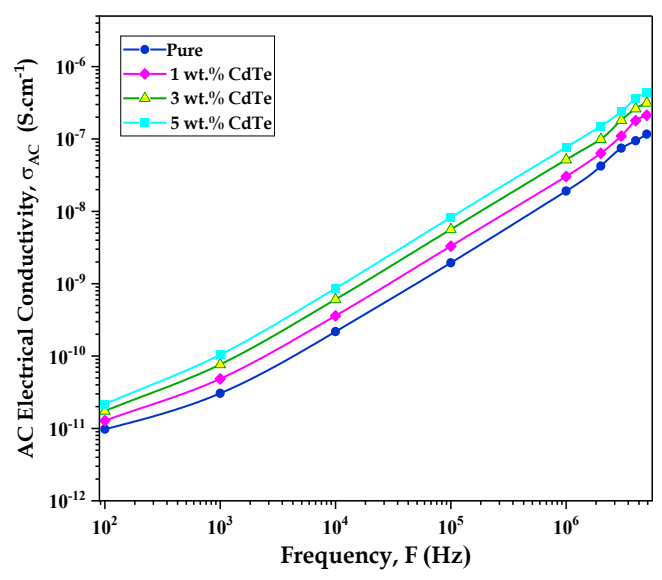


Figure 16. Frequency-dependent variation of AC electrical conductivity in (PVA/CdTe) nanocomposites at RT

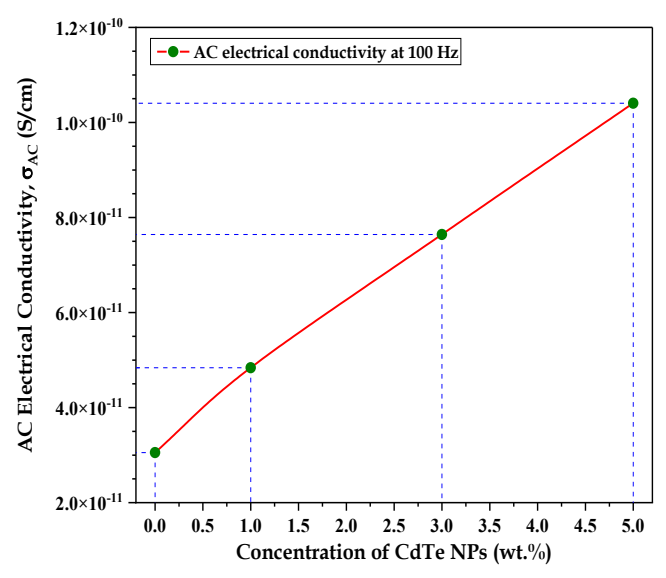


Figure 17. Effect of CdTe concentrations on A.C. electrical conductivity for (PVA/CdTe) nanocomposite at 100 Hz

4. CONCLUSION

This paper gives a short outline of a very good casting method that is used to make PVA/CdTe nanocomposites. Through FTIR research, it was shown that the PVA polymer matrix and CdTe NPs do interact in real ways. The findings show that there is a direct link between the amount of CdTe NPs in the PVA/CdTe nanocomposites' light absorbance, which causes the transmittance to decrease. When CdTe NPs were added to PVA polymers at a concentration of 5% by weight, their energy gap decreased. A direct association exists between CdTe nanoparticles and optical constants, such as optical conductivity, absorbance factor, extinction factor, the refractive index, and both the imaginary and real components of dielectric constants. The dielectric constant and dielectric loss are augmented with the frequency and concentration of CdTe nanoparticles. In contrast, the AC conductivity of electricity rises with increasing frequency and concentration of CdTe nanoparticles. Ultimately, these

findings indicate that the PVA/CdTe nanocomposite is suitable for application in photodetector devices.

ACKNOWLEDGMENTS

The authors sincerely acknowledge the College of Education for Pure Sciences, University of Babylon, Iraq, for providing the necessary facilities.

REFERENCES

- [1] N. Domun, H. Hadavinia, T. Zhang, T. Sainsbury, G. H. Liaghat, and S. Vahid, "Improving the fracture toughness and the strength of epoxy using nanomaterials a review of the current status," *Nanoscale*, vol. 7, no. 23, pp. 10294–10329, 2015, doi: 10.1039/C5NR01354B.
- [2] J. Parameswaranpillai, G. Joseph, K. P. Shinu, S. Jose, N. V Salim, and N. Hameed, "Development of hybrid composites for automotive applications: effect of addition of SEBS on the morphology, mechanical, viscoelastic, crystallization and thermal degradation properties of PP/PS-xGnP composites," RSC Adv., vol. 5, no. 33, pp. 25634-25641, 2015, doi: 10.1039/C4RA16637J.
- [3] P. Jyotishkumar, E. Logakis, S. M. George, J. Pionteck, L. Häussler, R. Haßler, P. Pissis, and S. Thomas, "Preparation and properties of multiwalled carbon nanotube/epoxy-amine composites," *J. Appl. Polym. Sci.*, vol. 127, no. 4, pp. 3063–3073, Feb. 2013, doi: 10.1002/app.37674.
- [4] W. Yao and S. Yu, "Synthesis of Semiconducting Functional Materials in Solution: From II-VI Semiconductor to Inorganic-Organic Hybrid Semiconductor Nanomaterials," *Adv. Funct. Mater.*, vol. 18, no. 21, pp. 3357–3366, Nov. 2008, doi: 10.1002/adfm.200800672.
- [5] B. P. Chandra, V. K. Chandra, and P. Jha, "Luminescence of II-VI Semiconductor Nanoparticles," *Solid State Phenom.*, vol. 222, pp. 1–65, Nov. 2014, doi: 10.4028/www.scientific.net/SSP.222.1.
- [6] I. Agool, N. Mohammed, and H. Abd Al-Meer, "Synthesis and Characterization of CdTe NPs Induced by Laser Ablation in Liquids," *J. Adv. Phys.*, vol. 6, no. 2, pp. 241–247, Jun. 2017, doi: 10.1166/jap.2017.1314.
- [7] H. Kamari, N. Al-Hada, E. Saion, A. Shaari, Z. Talib, M. Flaifel, and A. Ahmed, "Calcined Solution-Based PVP Influence on ZnO Semiconductor Nanoparticle Properties," *Crystals*, vol. 7, no. 2, p. 2, Feb. 2017, doi: 10.3390/cryst7020002.
- [8] M. K. Mohammed, G. Al-Dahash, and A. Al-Nafiey, "Fabrication and Characterization of the PMMA/G/Ag Nanocomposite by Pulsed Laser Ablation (PLAL)," *Nano Biomed. Eng.*, vol. 14, no. 1, Apr. 2022, doi: 10.5101/nbe.v14i1.p15-22.
- [9] G. Fussell, J. Thomas, J. Scanlon, A. Lowman, and M. Marcolongo, "The effect of protein-free versus protein-containing medium on the mechanical properties and uptake of ions of PVA/PVP hydrogels," *J. Biomater. Sci. Polym. Ed.*, vol. 16, no. 4, pp. 489–503, Jan. 2005, doi: 10.1163/1568562053700219.
- [10] K. Liu, Y. Li, F. Xu, Y. Zuo, L. Zhang, H. Wang, and J. Liao,

- "Graphite/poly (vinyl alcohol) hydrogel composite as porous ringy skirt for artificial cornea," *Mater. Sci. Eng. C*, vol. 29, no. 1, pp. 261–266, Jan. 2009, doi: 10.1016/j.msec.2008.06.023.
- [11] S. Mathew, A. D. Saran, B. Singh Bhardwaj, S. Ani Joseph, P. Radhakrishnan, V. P. N. Nampoori, C. P. G. Vallabhan, and J. R. Bellare, "Size dependent optical properties of the CdSe-CdS core-shell quantum dots in the strong confinement regime," *J. Appl. Phys.*, vol. 111, no. 7, p. 74312, Apr. 2012, doi: 10.1063/1.3702430.
- [12] H. Weickmann, J. C. Tiller, R. Thomann, and R. Mülhaupt, "Metallized Organoclays as New Intermediates for Aqueous Nanohybrid Dispersions, Nanohybrid Catalysts and Antimicrobial Polymer Hybrid Nanocomposites," *Macromol. Mater. Eng.*, vol. 290, no. 9, pp. 875–883, Sep. 2005, doi: 10.1002/mame.200500153.
- [13] B. N. S. Sooraj and T. Pradeep, "Optical properties of metal clusters," in *Atomically Precise Metal Nanoclusters*, vol. 25, Elsevier, 2023, pp. 83–101. doi: 10.1016/B978-0-323-90879-5.00010-X.
- [14] M. L. Sheqnab and R. S. Alnayli, "Effect Of Cdte Nanoparticles On Linear And Nonlinear Optical Property Of Polyvinyl Alcohols PVA Film," J. Coll. Educ. PURE Sci., vol. 9, no. 2, pp. 259–268, Jun. 2019, doi: 10.32792/utq.jceps.09.02.28.
- [15] Y. Liu *et al.*, "Structural Insight in the Interfacial Effect in Ferroelectric Polymer Nanocomposites," *Adv. Mater.*, vol. 32, no. 49, p. 2005431, Dec. 2020, doi: 10.1002/adma.202005431.
- [16] T. Shuvra Basu, S. Ghosh, S. Gierlotka, and M. Ray, "Collective charge transport in semiconductor-metal hybrid nanocomposite," *Appl. Phys. Lett.*, vol. 102, no. 5, p. 53107, Feb. 2013, doi: 10.1063/1.4790300.
- [17] A. Kharazmi, N. Faraji, R. Mat Hussin, E. Saion, W. M. M. Yunus, and K. Behzad, "Structural, optical, optothermal and thermal properties of ZnS–PVA nanofluids synthesized through a radiolytic approach," *Beilstein J. Nanotechnol.*, vol. 6, no. 1, pp. 529–536, Feb. 2015, doi: 10.3762/bjnano.6.55.
- [18] I. Jipa, A. Stoica, M. Stroescu, L.-M. Dobre, T. Dobre, S. Jinga, and C. Tardei, "Potassium sorbate release from poly(vinyl alcohol)-bacterial cellulose films," *Chem. Pap.*, vol. 66, no. 2, pp. 138–143, Jan. 2012, doi: 10.2478/s11696-011-0068-4.
- [19] H. Hendrawan, F. Khoerunnisa, Y. Sonjaya, and A. D. Putri, "Poly (vinyl alcohol)/glutaraldehyde/ Premna oblongifolia merr extract hydrogel for controlled-release and water absorption application," *IOP Conf. Ser. Mater. Sci. Eng.*, vol. 509, p. 012048, May 2019, doi: 10.1088/1757-899X/509/1/012048.
- [20] S. R. Manohara, and L. Gerward, "Influence of polyvinylpyrrolidone on optical, electrical, and dielectric properties of poly(2-ethyl-2-oxazoline)polyvinylpyrrolidone blends," *J. Mol. Liq.*, vol. 247, pp. 328–336, Dec. 2017, doi: 10.1016/j.molliq.2017.09.086.
- [21] A.N. Hadi, M.H. Meteab, and M. K. Mohammed, "Influence of Inclusion Sb2O3/NiO Nanostructures on the Morphological, Microstructural, and Optical Characteristics of PVA Polymeric for Gamma-Ray Shielding Applications," Rev. des Compos. des Matériaux

- *Avancés*, vol. 35, no. 3, p. 581, Jun. 2025, doi:10.18280/rcma.350319.
- [22] H. Ahmed and A. Hashim, "Design and characteristics of novel PVA/PEG/Y2O3 structure for optoelectronics devices," *J. Mol. Model.*, vol. 26, no. 8, p. 210, Aug. 2020, doi: 10.1007/s00894-020-04479-1.
- [23] R. S. Ali, M. K. Mohammed, A. A. Khadayeir, Z. M. Abood, N. F. Habubi, and S. S. Chiad, "Structural and Optical Characterization of Sprayed nanostructured Indium Doped Fe 2 O 3 Thin Films," *J. Phys. Conf. Ser.*, vol. 1664, no. 1, p. 012016, Nov. 2020, doi: 10.1088/1742-6596/1664/1/012016.
- [24] M. A. Morsi, A. H. Oraby, A. G. Elshahawy, and R. M. Abd El-Hady, "Preparation, structural analysis, morphological investigation and electrical properties of gold nanoparticles filled polyvinyl alcohol/carboxymethyl cellulose blend," *J. Mater. Res. Technol.*, vol. 8, no. 6, pp. 5996–6010, Nov. 2019, doi: 10.1016/j.jmrt.2019.09.074.
- [25] A. A. Jabber and A. R. Abdulridha, "Preparation and Characterization of CuO/ZnO Nanostructures Thin Films using Thermal Evaporation for Advanced Gas Sensing Applications," *Trends Sci.*, vol. 22, no. 3, p. 9002, Jan. 2025, doi: 10.48048/tis.2025.9002.
- [26] A. Y. Yassin, A. M. Abdelghany, R. S. Salama, and A. E. Tarabiah, "Structural, Optical and Antibacterial Activity Studies on CMC/PVA Blend Filled with Three Different Types of Green Synthesized ZnO Nanoparticles," J. Inorg. Organomet. Polym. Mater., vol. 33, no. 7, pp. 1855–1867, Jul. 2023, doi: 10.1007/s10904-023-02622-y.
- [27] M. M. Damoom, A. Saeed, E. M. Alshammari, A. M. Alhawsawi, A. Y. Yassin, J. A. M. Abdulwahed, and A. A. Al-Muntaser, "The role of TiO2 nanoparticles in enhancing the structural, optical, and electrical properties of PVA/PVP/CMC ternary polymer blend: nanocomposites for capacitive energy storage," *J. Sol-Gel Sci. Technol.*, vol. 108, no. 3, pp. 742–755, Dec. 2023, doi: 10.1007/s10971-023-06223-6.
- [28] M. Jukić, I. Sviben, Z. Zorić, and S. Milardović, "Effect of Polyvinylpyrrolidone on the Formation AgBr Grains in Gelatine Media," *Croat. Chem. Acta*, vol. 85, no. 3, pp. 269–276, 2012, doi: 10.5562/cca1919.
- [29] N. Rajeswari, S. Selvasekarapandian, S. Karthikeyan, M. Prabu, G. Hirankumar, H. Nithya, and C. Sanjeeviraja, "Conductivity and dielectric properties of polyvinyl alcohol-polyvinylpyrrolidone poly blend film using non-aqueous medium," *J. Non. Cryst. Solids*, vol. 357, no. 22–23, pp. 3751–3756, Nov. 2011, doi: 10.1016/j.jnoncrysol.2011.07.037.
- [30] M. K. Mohammed, M. H. Abbas, A. Hashim, B. H. Rabee, M. A. Habeeb, and N. Hamid, "Enhancement of Optical Parameters for PVA/PEG/Cr2O3 Nanocomposites for Photonics Fields," *Rev. des Compos. des Mater. Av.*, vol. 32, no. 4, pp. 205–209, 2022, doi: 10.18280/rcma.320406.
- [31] M. K. Mohammed, T. N. Khudhair, K. S. Sharba, A. Hashim, Q. M. Hadi, and M. H. Meteab, "Tuning the Morphological and Optical Characteristics of SnO2/ZrO2 Nanomaterials Doped PEO for Promising Optoelectronics Applications," Rev. des Compos. des Matériaux Avancés, vol. 34, no. 4, pp. 495–503, Aug.

- 2024, doi: 10.18280/rcma.340411.
- [32] A. Rahma, M. M. Munir, Khairurrijal, A. Prasetyo, V. Suendo, and H. Rachmawati, "Intermolecular Interactions and the Release Pattern of Electrospun Curcumin-Polyvinyl(pyrrolidone) Fiber," *Biol. Pharm. Bull.*, vol. 39, no. 2, pp. 163–173, 2016, doi: 10.1248/bpb.b15-00391.
- [33] L. K. Mireles, M.-R. Wu, N. Saadeh, L. Yahia, and E. Sacher, "Physicochemical Characterization of Polyvinyl Pyrrolidone: A Tale of Two Polyvinyl Pyrrolidones," ACS Omega, vol. 5, no. 47, pp. 30461–30467, Dec. 2020, doi: 10.1021/acsomega.0c04010.
- [34] T. S. Soliman, S. A. Vshivkov, and S. I. Elkalashy, "Structural, thermal, and linear optical properties of <scp> SiO 2 </scp> nanoparticles dispersed in polyvinyl alcohol nanocomposite films," *Polym. Compos.*, vol. 41, no. 8, pp. 3340–3350, Aug. 2020, doi: 10.1002/pc.25623.
- [35] J. Fal, K. Bulanda, J. Traciak, J. Sobczak, R. Kuzioła, K. M. Grąz, G. Budzik, M. Oleksy, and G. Żyła, "Electrical and Optical Properties of Silicon Oxide Lignin Polylactide (SiO2-L-PLA)," *Molecules*, vol. 25, no. 6, p. 1354, Mar. 2020, doi: 10.3390/molecules25061354.
- [36] S. R. Sahib and B. H. Rabee, "Production of a versatile PMMA/PEO-CuO-In2O3 nanocomposite with its characterization, cold plasma treatment, and applications for flexible emission filter devices and smart moisture," *Nano-Structures & Nano-Objects*, vol. 40, p. 101382, Dec. 2024, doi: 10.1016/j.nanoso.2024.101382.
- [37] A. Paydayesh, A. A. Azar, and A. J. Arani, "Investigation the effect of Graphene on The Morphology, Mechanical and Thermal properties of PLA/PMMA Blends," *Ciência e Nat.*, vol. 37, no. 6–1, p. 15, Dec. 2015, doi: 10.5902/2179460X20823.
- [38] N.A. Sami, A.M. Nattah, R.A. Jawad, M.H. Meteab, and M.K. Mohammed, "Modification and Enhancement of The Structural, Morphological and Optical Characteristics of PMMA/In2O3/SiO2 Promising Ternary Nanostructures for Optical Nanodevices and Gamma Ray Attenuation," *Trends Sci.*, vol. 22, no. 7, p. 9959, May. 2025, doi:10.48048/tis.2025.9959.
- [39] S. R. Sahib and B. H. Rabee, "Synthesizing, characterizing, and cold plasma treating of Cr2O3/CuO nanomaterials doped PMMA/PEO for flexible optoelectronic applications," *Opt. Mater. (Amst).*, vol. 157, p. 116139, 2024, doi: 10.1016/j.optmat.2024.116139.
- [40] F. M. Nayef and B. H. Rabee, "Effect of plasma irradiation on the electrical characteristics of the PMMA-PS/Al2O3 nanocomposites," *Dig. J. Nanomater. Biostructures*, vol. 18, no. 2, pp. 669–680, 2023, doi: 10.15251/DJNB.2023.182.669.
- [41] H. K. Jaafar, A. Hashim, and B. H. Rabee, "Fabrication and unraveling the morphological, structural, and dielectric features of PMMA-PEO-SiC-BaTiO3 promising quaternary nanocomposites for multifunctional nanoelectronics applications," *J. Mater. Sci. Mater. Electron.*, vol. 35, no. 2, p. 128, 2024, doi: 10.1007/s10854-024-11924-x.
- [42] H. Shivashankar, K. A. Mathias, P. R. Sondar, M. H. Shrishail, and S. M. Kulkarni, "Study on low-frequency

- dielectric behavior of the carbon black/polymer nanocomposite," *J. Mater. Sci. Mater. Electron.*, vol. 32, no. 24, pp. 28674–28686, Dec. 2021, doi: 10.1007/s10854-021-07242-1.
- [43] A. M. El Sayed and S. El-Gamal, "Synthesis and investigation of the electrical and dielectric properties of Co3O4/(CMC+PVA) nanocomposite films," *J. Polym. Res.*, vol. 22, no. 5, p. 97, May 2015, doi: 10.1007/s10965-015-0732-4.
- [44] L. S. R. Yadav, B. Archana, K. Lingaraju, C. Kavitha, D. Suresh, H. Nagabhushana, and G. Nagaraju, "Electrochemical Sensing, Photocatalytic and Biological Activities of ZnO Nanoparticles: Synthesis
- via Green Chemistry Route," *Int. J. Nanosci.*, vol. 15, no. 04, p. 1650013, Aug. 2016, doi: 10.1142/S0219581X16500137.
- [45] S. Tewari, A. Bhattacharjee, and P. P. Sahay, "Structural, dielectric, and electrical studies on thermally evaporated CdTe thin films," *J. Mater. Sci.*, vol. 44, no. 2, pp. 534–540, 2009, doi: 10.1007/s10853-008-3088-x.
- [46] Pooja and P. Chowdhury, "Optical and electronic properties of CdTe quantum dots in their freezed solid matrix phase and solution phase," *Mater. Today Proc.*, vol. 28, pp. 201–204, 2020, doi: 10.1016/j.matpr.2020.01.561.